An Analytical and Experimental Investigation of Annular Propulsive Nozzles

Ralph R. Conley*
McDonnell Douglas Astronautics Company, St. Louis, Missouri
and
Joe D. Hoffman† and H. Doyle Thompson‡
Purdue University, West Lafayette, Indiana

This paper discusses an analytical performance prediction methodology for annular propulsive nozzles and the application of that methodology to selected nozzles. Thrust efficiencies and static pressure profiles from cold-flow testing of the selected nozzles are summarized and compared to the predictions. These comparisons show that the analytical methods are reasonably accurate if the radial velocity components in the transonic region of annular nozzles are small. The areas of prediction/test disagreement are identified for future improvements.

Nomenclature

IVL = initial-value line
MOC = method of characteristics
NPR = nozzle pressure ratio
VNAP = viscous nozzle analysis program
VNAP2 = viscous nozzle analysis program, version 2

Introduction

THE conventional propulsive nozzle is an axisymmetric converging-diverging design and has been used successfully in rocket, turbojet, and ramjet engines for many years. The advantages of such nozzles include efficient design point performance, reasonable weight and cost, and the availability of accurate design/analysis techniques. On the other hand, the disadvantages of such nozzles include excessive length and inefficient off-design performance.

Several annular nozzle concepts, formed by inserting axisymmetric centerbodies within conventional nozzles, have been considered to overcome these disadvantages. As depicted in Fig. 1, the centerbody may be located either upstream, downstream, or in the throat plane of the conventional nozzle. The objective of the present work was to conduct analytical and experimental investigations of selected annular nozzles to acquire a better understanding of the flow processes and performance potential of these concepts.

This paper presents the results of this work for five annular nozzles encompassing the design options noted in Fig. 1. Primary emphasis is on an analytical performance prediction methodology for such nozzles and the application of that methodology. The results of considerable cold-flow testing of selected nozzle models are summarized and compared with the analytical predictions. The areas of prediction/test disagreement are identified for future improvements.

Cold-Flow Testing

Annular nozzle model cold-flow testing was conducted in the McDonnell Aircraft Company Nozzle Test Stand facility. A complete description of this test facility, including assessments of pressure ratio capability and thrust measurement accuracy, is given in Ref. 1.

Four annular nozzles encompassing the design options noted in Fig. 1 were selected for model fabrication and cold-flow testing. The internal contours of these nozzles were developed by various design techniques.[2,3] An additional nozzle model was also fabricated based on a design improvement study described later in this paper. All nozzle models included provisions for measuring the cowl static pressure at several axial stations. An average of four cold-flow test runs were made for each model. Thrust, mass flow rate, and cowl static pressure data were recorded at 8-10 values of nozzle pressure ratio for each run.

Nozzle Efficiency

The nozzle thrust efficiency employed in the present study is the pressure ratio efficiency, which compares the actual nozzle thrust to the ideal thrust obtained by expanding the actual mass flow rate from the nozzle stagnation pressure to the ambient pressure. Since the ideal thrust is that developed by isentropic expansion over the pressure ratio, it is independent of the nozzle geometric design.

This definition of nozzle efficiency is used throughout this study. For the measured efficiency, the actual thrust and mass flow rate are the measured values. For the predicted efficiency, the actual thrust and mass flow rate are the predicted values obtained with the analytical methods discussed in the next section. The ideal thrust for either efficiency is calculated from the appropriate actual mass flow rate and pressure ratio.

Performance Prediction Methodology

The accuracy and effectiveness of nozzle performance prediction techniques are highly dependent on the flowfield model chosen to represent the actual flowfield. In the present study, the flowfield model is based on the following assumptions: 1) steady axisymmetric flow, 2) inviscid nonconducting fluid with no body forces, 3) thermally and calorically perfect gas, and 4) separation and base pressures selected from empirical correlations. The governing equations consist of the continuity equation, component momentum equations, energy equation, and thermal and caloric equations of state. A detailed discussion of these equations is presented in Ref. 4.

The choice of a numerical method, or methods, to solve these governing equations is also crucial to the success of the performance prediction procedure. A subsonic/transonic solution is required to define the throat thrust, while a super-

Presented as Paper 84-0282 at the AIAA 22nd Aerospace Sciences Meeting, Reno, Nev., Jan. 9-12, 1984; received March 9, 1984; revision received Jan. 10, 1985.

*Technical Specialist. Member AIAA.
†Professor of Mechanical Engineering. Member AIAA.
‡Professor of Mechanical Engineering. Associate Fellow AIAA.

sonic solution is required to define the thrusts developed by the cowl and centerbody. Experience has shown that subsonic/transonic flowfields can be adequately determined by finite difference approaches, whereas the method of characteristics is the most accurate approach to determining supersonic flowfields in nozzles.

The numerical methods selected for the performance prediction procedure are a finite difference approach, as employed in the VNAP code,[5] to define the subsonic/transonic flowfield and a method of characteristics approach, denoted as the MOC code,[6] to define the supersonic flowfield. The VNAP code solves the governing equations for unsteady flow using MacCormack's finite difference scheme[7] and the steady-state flowfield is obtained as the asymptotic solution at large time. The VNAP code was used primarily as an inviscid code in this study. The viscous capabilities of this code were employed only when necessary to capture shock waves. As noted in subsequent discussions, the more recent VNAP2 code[8] provides superior results and is recommended for future studies.

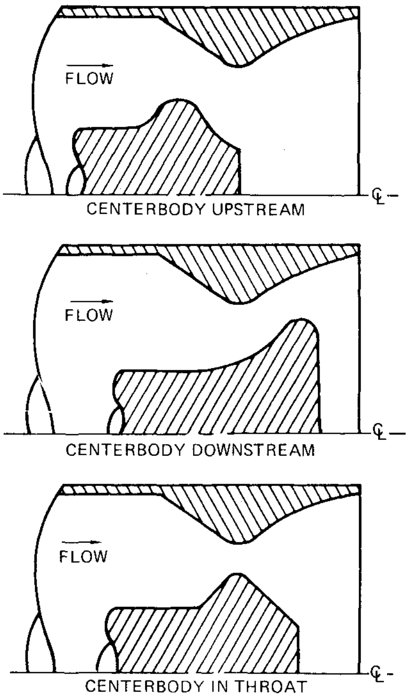

Fig. 1 Annular nozzle concepts.

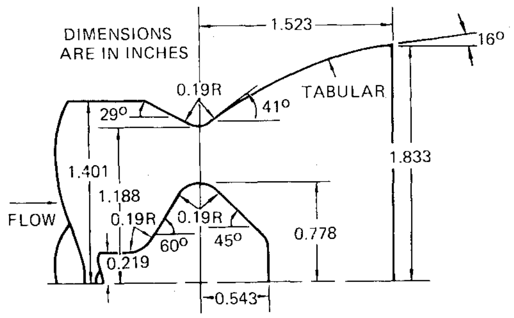

Fig. 2 Geometry of nozzle N1.

Performance Prediction Example

The application of the selected performance prediction methodology to nozzle N1 (see Fig. 2) is presented in this section. The flowfield solutions obtained from the VNAP and MOC codes are presented and the calculations of the throat, cowl, and centerbody thrusts are described in detail. Comparisons with cold-flow test data are also made.

Nozzle N1, depicted in Fig. 2, has an axisymmetric cowl consisting of a cylindrical upstream section, a conical-circular arc shoulder section, and a contoured downstream section. The axisymmetric centerbody has a cylindrical upstream support section, a conical initial section, a circular arc shoulder, a conical section downstream of the shoulder, and a flat aft-facing base. Note that the shoulder sections of the cowl and centerbody are at the same axial station.

As previously mentioned, the subsonic/transonic solution obtained from the VNAP code defines the nozzle throat flowfield. Figure 3 illustrates the Mach number distribution in the throat region of nozzle N1 as an example of the flowfield definition provided by the VNAP code. From this definition, the throat thrust is determined by integrating the momentum flux and pressure forces across a selected line that spans the throat in the slightly supersonic region. This same line, denoted as the initial-value line (IVL), is then used to start the MOC code solution of the supersonic flowfield.

The thrusts developed by the pressures acting on the cowl and centerbody surfaces are determined by integrating the axial components of the pressure forces acting on these surfaces. The pressure distributions along the cowl and centerbody surfaces are obtained from the supersonic flowfield solution provided by the MOC code. The MOC code constructs the flowfield solution along the previously mentioned IVL, beginning at the cowl and proceeding along the IVL to the centerbody surface. The code continues the solution along the centerbody surface until a specified separation pressure is reached. At this point, a free-pressure boundary is initiated and tracked downstream. Left-running Mach lines emanating from these boundaries are propagated across the flowfield to the cowl. The Mach lines are allowed to cross and fold over, simulating the occurrence of embedded oblique shock waves. This procedure is continued until the entire cowl and centerbody wall pressure distributions have been determined. Figure 4 illustrates the left-running Mach lines in the supersonic flowfield of nozzle N1 as an example of the MOC code solution. Note the occurrence of a mild right-running oblique shock wave in this nozzle.

An alternative to the throat flowfield defined by the VNAP code is to simply assume the geometry of a slightly supersonic, constant Mach number line that spans the nozzle throat. This uniform IVL is then treated in the same manner as the VNAP-defined IVL for throat thrust calculations and MOC code usage. As will be shown, this alternative procedure provides good results if the throat flowfield is reasonably uniform.

The predicted and measured cowl pressure distributions for nozzle N1 are presented in Fig. 5. Note that the logarithmic pressure ratio scale accentuates the differences between the predicted and measured pressures. The predicted pressures are presented for two IVL's: the IVL determined from the VNAP code and a uniform IVL with a constant Mach number of 1.02. The two predicted pressure distributions are reasonably close, indicating that the subsonic/transonic flowfield is fairly uniform. The Mach number distributions previously presented in Fig. 4 support that conclusion. The predicted pressure distribution agrees well with the measured pressures except in the region just downstream of the cowl shoulder where the predicted pressure rise is more rapid than the measured rise.

The cowl and centerbody base thrusts are computed by assuming that a uniform pressure acts over these base areas. Base pressures must be estimated from empirical correlations. In the present investigation, the cowl base pressure was equated to the ambient pressure. Based on a limited amount of experimental data,[9] the centerbody base pressure was assumed to be 5% of the nozzle chamber stagnation pressure.

The predicted and measured values of the nozzle pressure ratio efficiency are presented in Fig. 6. The trend of measured efficiency as a function of nozzle pressure ratio follows the predicted trend very closely. The magnitude of the predicted efficiency is approximately 1% less than the measured effi-

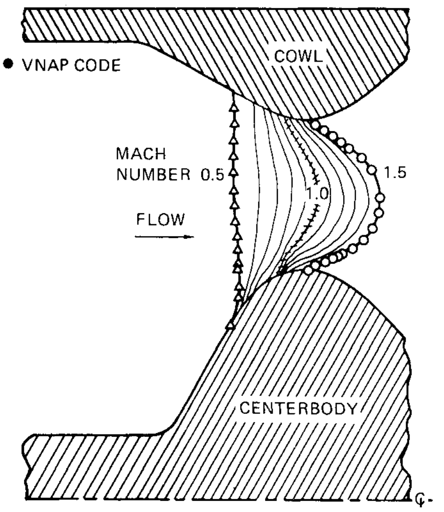

Fig. 3 Mach number distribution for nozzle N1.

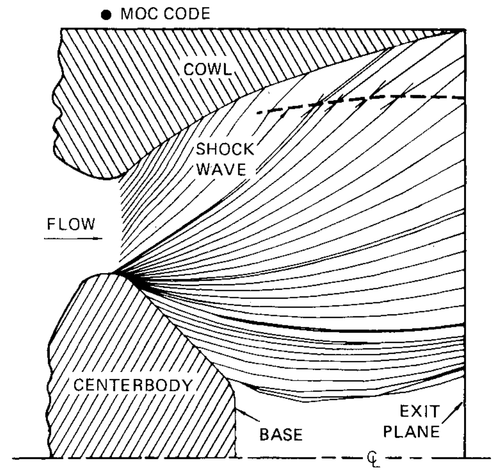

Fig. 4 Left-running Mach lines for nozzle N1.

ciency, which is considered to be very good agreement. These results demonstrate that the selected performance prediction methodology is capable of accurately predicting the flowfield and performance of annular nozzles.

Results

The results of the flowfield analysis, performance prediction, and experimental testing of three other annular nozzle configurations are presented in this section. These three nozzles, which have their centerbodies located downstream, upstream, and in the throat plane, exercise the capabilities of the methodology and illustrate its strengths and weaknesses.

Nozzle N2

Nozzle N2, depicted in Fig. 7, has an axisymmetric cowl consisting of a cylindrical upstream section, a conical-circular arc shoulder section, and a contoured downstream section. The axisymmetric centerbody has a cylindrical upstream support section, a conical initial section, a circular arc shoulder section, a conical section downstream of the shoulder, and a flat aft-facing base. Note that the centerbody shoulder is downstream of the cowl shoulder.

Figure 8 presents the Mach number distribution obtained by the VNAP code for this nozzle. The flowfield is highly distorted in the transonic region. The Mach number contours show a rapid expansion around the cowl shoulder, with the Mach number reaching values larger than 1.5. This highly supersonic region is followed by a rapid compression that causes the flow to go subsonic on the cowl. This compression is caused by the rapid inward turning of the cowl contour, coupled with the considerable radially outward momentum in the transonic flowfield.

A slightly supersonic IVL was selected from the VNAP code results and used to start the MOC code solution of the supersonic flowfield. The computed flow became subsonic on the cowl and the MOC code aborted at an axial location corresponding to the subsonic pocket shown in Fig. 8.

Attempts were made to obtain a supersonic solution by starting the MOC code with a uniform IVL across the nozzle geometric throat (i.e., the conic surface defined by the line connecting the center of curvature of the cowl shoulder and the center of curvature of the centerbody shoulder) for Mach numbers of 1.01 and 1.02. Both attempts resulted in MOC code aborts due to the computed flow becoming subsonic on the cowl. However, for a Mach number of 1.03, the flow remained supersonic and a flowfield solution was obtained.

Figure 9 presents the pressure distributions on the cowl obtained from the MOC solution for the uniform IVL and the

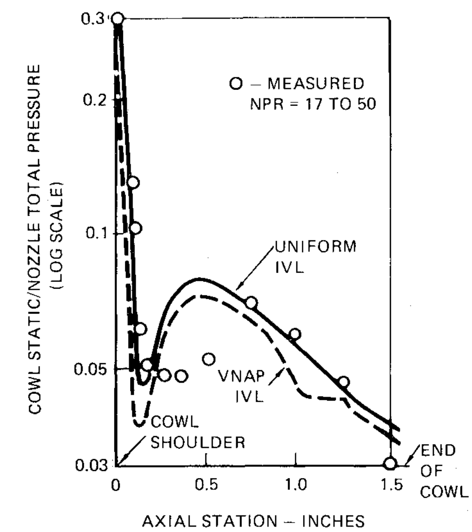

Fig. 5 Cowl pressures for nozzle N1.

VNAP IVL. For the uniform IVL solution, the initial expansion is followed immediately by a strong compression that decelerates the flow to only a slightly supersonic Mach number. Downstream of the nearly constant-pressure region, the pressure drops smoothly. For the VNAP IVL, the flow initially expands to a lower pressure because of the effects of the upstream geometry. The recompression then results in a subsonic flow region that causes the MOC code to abort. The experimental measurements of static pressure on the cowl, also presented in Fig. 9, indicate that the initial expansion is more rapid than the uniform IVL solution predicts, but not as rapid as the VNAP IVL solution indicates. The recompression is clearly indicated, but the flow apparently remains supersonic. Note that the predicted and measured pressures agree well at more downstream cowl locations.

Cline[10] analyzed nozzle N2 with the VNAP code and obtained the same results presented in Fig. 9. He concluded that the lack of agreement in the pressure distribution just downstream of the throat is due mainly to the small throat radius of curvature and subsequent flow separation.

The predicted and measured nozzle efficiencies for nozzle N2 are compared in Fig. 10. The dual values of measured efficiencies at lower pressure ratios are due to centerbody wake structure changes, which were determined by exit plane pitot pressure surveys not discussed in this paper. At higher pressure ratios, the predicted efficiencies are approximately 2% higher than the measured values. This difference could be

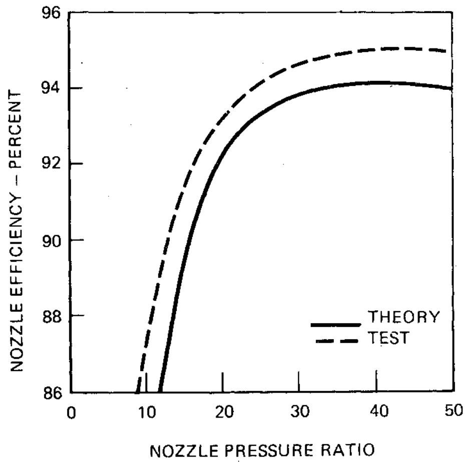

Fig. 6 Efficiency comparison for nozzle N1.

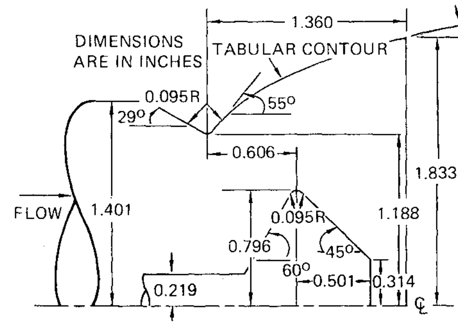

Fig. 7 Geometry of nozzle N2.

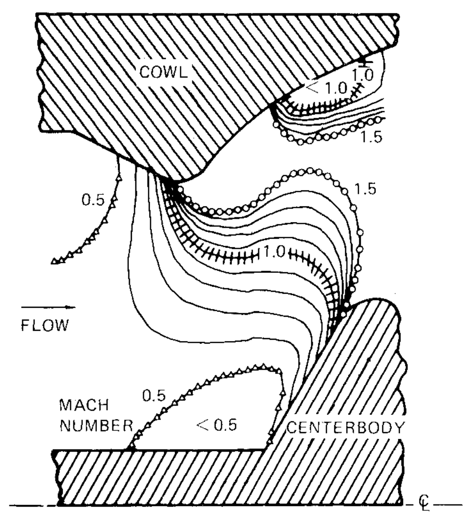

Fig. 8 Mach number distribution for nozzle N2.

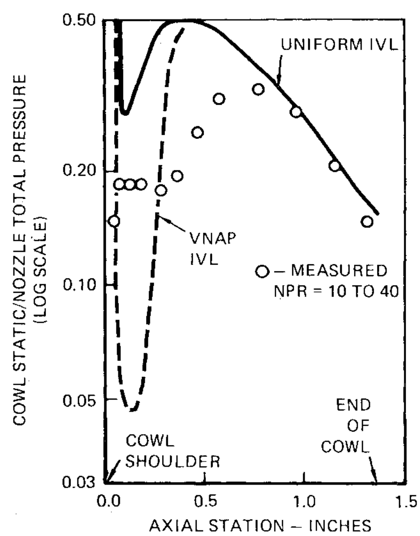

Fig. 9 Cowl pressures for nozzle N2.

anticipated, since the predicted cowl pressures (Fig. 9) are generally higher than the measured pressures. The inability to more accurately analyze such flowfields is identified as a major deficiency in the state-of-the-art of nozzle flowfield analysis.

Nozzle N3

Nozzle N3, depicted in Fig. 11, has an axisymmetric cowl consisting of a cylindrical upstream section, a conical-circular arc shoulder section, and a conical downstream section. The axisymmetric centerbody has a cylindrical upstream support section, a conical initial section, a circular arc shoulder section, a contoured section downstream of the shoulder, and a flat aft-facing base. Like nozzle N1, the shoulders of the centerbody and cowl are at the same axial station.

The Mach number contours and Mach lines obtained by the VNAP and MOC codes are not presented, since they are very similar to those previously shown in Figs. 3 and 4 for nozzle N1. Figure 12 compares the predicted and measured pressure distributions on the cowl for both the uniform IVL and the VNAP IVL solutions with the MOC code. The predicted pressure distributions are almost identical and compare very well with the measured pressures.

Figure 13 compares the predicted and measured nozzle efficiencies for nozzle N3. The agreement is very good at higher nozzle pressure ratios. The increased difference between the predicted and measured efficiencies at lower nozzle pressure ratios is due to flow separation near the cowl exit, as determined by cowl pressure measurements not discussed in this paper.

Nozzle N4

Nozzle N4 is a rearrangement of nozzle N3 model components that locates the centerbody shoulder upstream of the cowl shoulder. This configuration completes the annular nozzle design options noted in Fig. 1. The resulting geometry for nozzle N4 is illustrated in Fig. 14.

The transonic Mach number distribution obtained from the VNAP code is presented in Fig. 15 and depicts a highly distorted flowfield. A region of locally supersonic flow occurs at the centerbody shoulder. The flow downstream of this region recompresses and remains subsonic all the way to the nozzle axis. Since it was necessary to assume an extension to the centerbody for the VNAP code analysis, it was hypothesized that the assumed extension geometry influenced the results. Several different centerbody extension contours were evaluated in an attempt to obtain supersonic flow on the centerbody or its extension. However, with the exception of the previously mentioned supersonic pocket at the shoulder, the flow remained subsonic all the way to the nozzle axis for reasonable extension geometries.

A slightly supersonic IVL was selected from the VNAP code results and used to start the MOC code solution of the supersonic flowfield. The predicted pressure distribution on the cowl is compared with the measured pressures in Fig. 16. The predicted pressures in the supersonic region downstream of the cowl shoulder do not show the degree of expansion indicated by the measured values.

Attempts were made to start the MOC code solution with a uniform IVL across the nozzle geometric throat. Due to the centerbody design, this minimum flow area for nozzle N4 is a

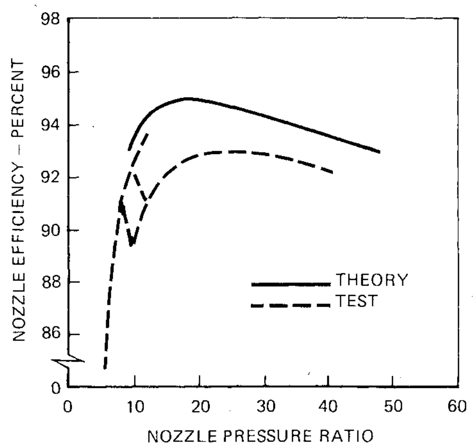

Fig. 10 Efficiency comparison for nozzle N2.

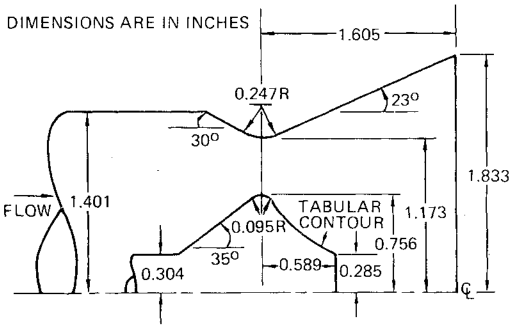

Fig. 11 Geometry of nozzle N3.

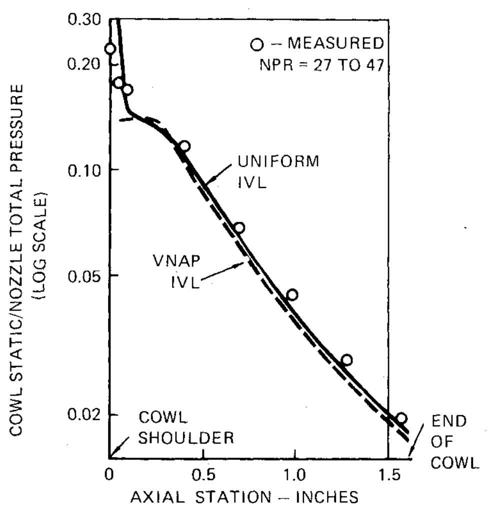

Fig. 12 Cowl pressures for nozzle N3.

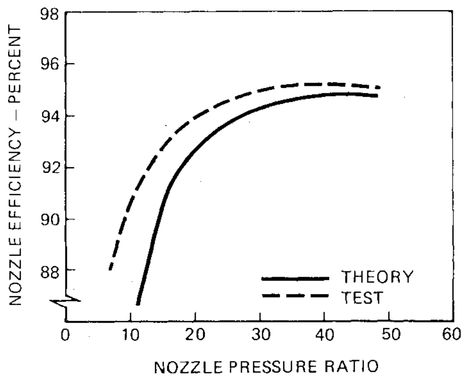

Fig. 13 Efficiency comparison for nozzle N3.

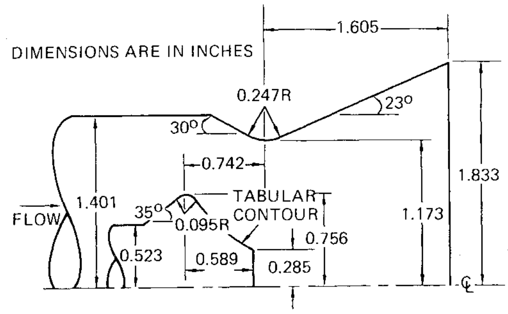

Fig. 14 Geometry of nozzle N4.

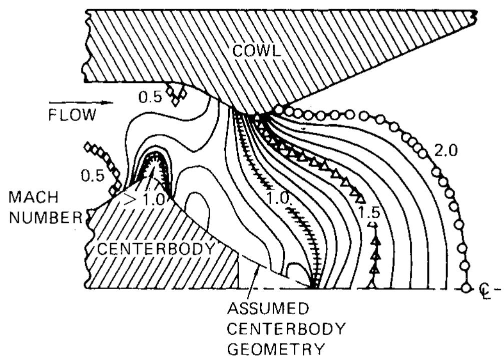

Fig. 15 Mach number distribution for nozzle N4.

conic surface defined by a line connecting the center of curvature of the cowl shoulder with the edge of the centerbody base. These attempts were unsuccessful due to the computed flow becoming subsonic. As an alternative, the VNAP code was then used to obtain a solution for the entire nozzle flowfield. Figure 16 shows that the pressures predicted by this VNAP solution agree very well with the measured values in the subsonic region upstream of the cowl shoulder. However, in the supersonic flow region downstream of the shoulder, the agreement is poorer than the predictions obtained with the MOC code using the VNAP IVL.

Cline[10] analyzed the VNAP code results presented in Figs. 15 and 16 and concluded that the numerical smoothing approach employed in the present study to account for shocks in the supersonic pocket at the centerbody shoulder was inappropriate. He corrected this and obtained the predicted cowl pressures presented in Fig. 16. As shown, these predictions are considerably better than the original. Cline also analyzed this nozzle with the VNAP2 code and the predicted cowl pressures are shown in Fig. 16. These latter predictions are superior to both VNAP code predictions because the VNAP2 code does a much better job of calculating shock waves in the previously mentioned supersonic pocket.

Figure 17 compares the predicted and measured nozzle efficiencies for nozzle N4. The discontinuity in the measured efficiency curve near a pressure ratio of 8:1 is due to flow separation. At higher pressure ratios, the predicted efficiencies are approximately 3% larger than measured. This is attributed to the mismatch between the predicted and measured cowl pressure distributions, as previously discussed.

Design Improvement Study

The analytical methods described in this paper provide information that can be used to understand the nozzle flowfield and propose design changes for improved performance. The

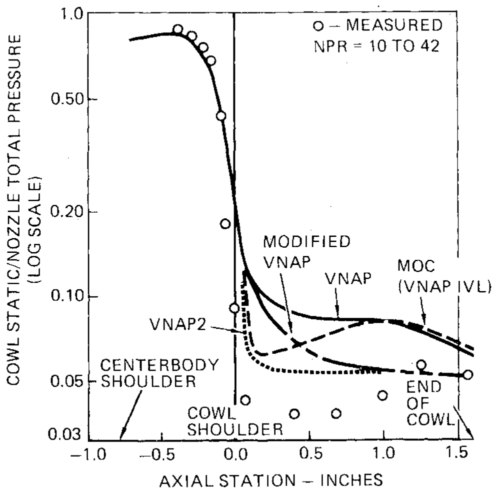

Fig. 16 Cowl pressures for nozzle N4.

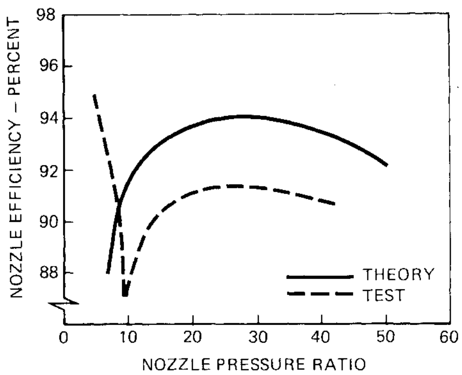

Fig. 17 Efficiency comparison for nozzle N4.

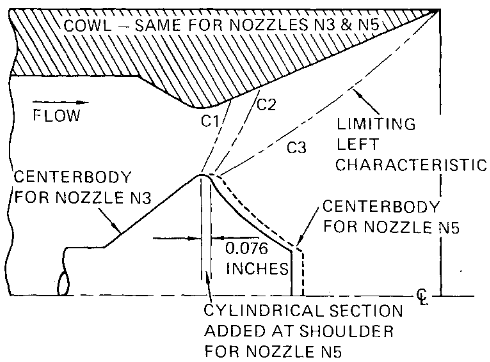

Fig. 18 Geometry of nozzle N5.

analysis also provides an inexpensive alternative to experimental comparisons of the proposed design variants. As an example, this section summarizes a limited study to improve the performance of nozzle N3 through small changes to the cowl and centerbody contours. Nozzle N3 was selected since it exhibited good predicted performance and a high degree of confidence exists in the analytical methods for this configuration. The subsonic contour of the nozzle was not altered in this study and all computations were made using the MOC code. A uniform IVL with a Mach number of 1.02 at the minimum geometric area was used to start the MOC code solution.

Three design changes to the cowl and centerbody were investigated. These changes and the predicted results were:

1) Replacing the aft contoured section of the centerbody with a conical section would result in a small performance decrease.

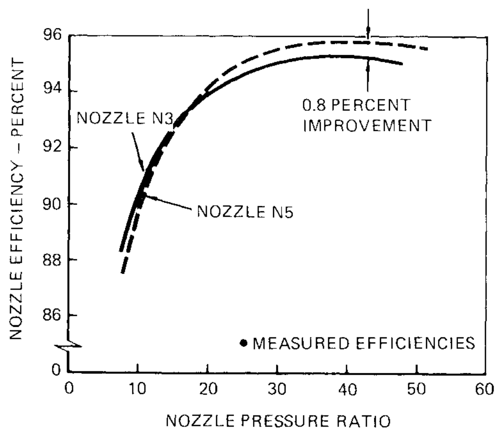

Fig. 19 Efficiency improvement with design change.

2) Replacing the conical cowl with a parabolic contour would result in a slight performance increase (about 0.2%).

3) Adding a short cylindrical section to the centerbody would result in a modest performance increase (about 0.8%).

Design change 3 was selected for testing since it offered the greatest potential for performance improvement. This nozzle is denoted as N5 and is depicted in Fig. 18. The measured thrust efficiencies for nozzle N5 and those for the reference nozzle N3 are compared in Fig. 19. This comparison verifies the predicted performance increase and confirms that analytical prediction techniques can be used to assess design changes for performance improvements.

The payoff in adding the cylindrical section to the centerbody can be explained in terms of cowl pressures by observing the characteristic wave pattern, also illustrated in Fig. 18. The pressure distribution on the cowl is primarily determined by expansion waves emanating from the centerbody surface just downstream of characteristic C1, which originates at the intersection of the centerbody and the IVL. These strong expansion waves, represented by characteristic C2 in Fig. 18, are generated by the rapid turning of the flow around the centerbody shoulder and cause a rapid decrease in the pressure on the cowl. Adding a short cylindrical section to the shoulder of the centerbody delays the turning of the flow and thus translates the attendant pressure decrease on the cowl further downstream. Further study of the characteristic pattern in Fig. 18 also reveals the limiting length of the cylindrical section to achieve performance benefits. Since characteristic C3 intersects the end of the cowl, changes to the centerbody downstream of its emanation point have no effect on the cowl pressure.

Summary and Conclusions

The analytical methods described in this paper are reasonably accurate for annular nozzles if the radial velocity components in the transonic region are small. The analytical methods provide valuable quantitative information that can be effectively used to understand the flowfield and generate ideas for design improvement. Furthermore, the methods are sufficiently accurate that the effects of small differences in designs can be accurately evaluated, thus reducing the amount of experimental work required to optimize a given design concept.

However, there are some deficiencies in the analytical capability for some annular nozzle flowfields. These include inadequate transonic flow analysis capability for flows with large radial velocity components, inability to treat strong shock waves (particularly when the shock waves produce subsonic pockets in the supersonic flowfield), very poor base pressure prediction methods, and inability to predict and calculate separated flows. Future improvements in these areas would enhance the analytical capability for annular nozzle flowfield prediction.

Acknowledgments

This work was performed under Contract F33615-80-C-2029 with the Aero Propulsion Laboratory, Air Force Wright Aeronautical Laboratories, Wright-Patterson Air Force Base, Ohio. Mr. J. R. Smith is the Air Force Project Engineer.

The analytical work was critically reviewed by Dr. Michael C. Cline of the Los Alamos Scientific Laboratory, Los Alamos, N. Mex. His numerous suggestions, which contributed to a better understanding of the analytical model, are sincerely appreciated.

References

[1]Conley, R. R., "High Pressure Ratio Testing with a Nozzle Driven Ejector," AIAA Paper 84-1488, June 1984.

[2]Rao, G. V. R., "Exhaust Nozzle Contour for Optimum Thrust," *Jet Propulsion*, Vol. 28, June 1958, pp. 377-382.

[3]Schorr, C. J. and McKenna, R. F., "Constant Chamber Pressure Throttling of an Expansion-Deflection Nozzle," AIAA Paper 69-435, June 1969.

[4]Zucrow, M. J. and Hoffman, J. D., *Gas Dynamics*, Vol. 1, John Wiley & Sons, New York, 1975, Chap. 10.

[5]Cline, M. C., "VNAP: A Computer Program for Computation of Two-Dimensional, Time-Dependent Compressible, Viscous, Internal Flow," Los Alamos Scientific Laboratory, Los Alamos, N. Mex., Rept. LA-7326, Nov. 1978.

[6]Thompson, H. D., "A Method of Characteristics Program for Computing Annular Nozzle Flowfields," Thermal Sciences and Propulsion Center, Purdue University, West Lafayette, Ind., Rept. ME-TSPC-83-05, June 1983.

[7]MacCormack, R. W., "The Effect of Viscosity in Hypervelocity Impact Cratering," AIAA Paper 69-354, April 1969.

[8]Cline, M. C., "VNAP2: A Computer Program for Computation of Two-Dimensional, Time-Dependent Compressible, Turbulent Flow," Los Alamos Scientific Laboratory, Los Alamos, N. Mex., Rept. LA-8872, Aug. 1981.

[9]Conley, R. R., Unpublished data, Sept. 1981.

[10]Cline, M. C., Private communication, March 1984.